RSC Advances

PAPER

View Article Online
View Journal | View Issue

Cite this: *RSC Adv.*, 2025, **15**, 23772

Determination of eight benzene homologues in airport ambient air and aircraft cabin air by two-stage thermal desorption-gas chromatography†

Tao Liu,‡[a] Tiankuo Yang,‡[a] Xiaoxue Yuan,[*b] Qingmin Su,[c] Jun Feng[d] and Jiwen Jiang*[a]

In this study, a two-stage thermal desorption-gas chromatography (TTD-GC) method was established to determine eight benzene homologues (benzene, toluene, ethylbenzene, *p*-xylene, *m*-xylene, *o*-xylene, styrene, and *p*-*tert*-butyltoluene) in airport ambient air and aircraft cabin air. By optimizing chromatographic conditions and two-stage thermal desorption parameters, detection sensitivity was significantly enhanced. The detection limits for the eight benzene homologues ranged from 41 ng m^{-3} to 108 ng m^{-3}, achieving sub-nanogram-level sensitivity, which enabled effective detection of low-concentration benzene homologues. The results demonstrated that the method was highly suitable for complex environmental samples, enabling effective separation and detection of the eight benzene homologues without interference from multiple substances in airport ambient air or other organic compounds released from cabin materials. Furthermore, the integrated design of sample pretreatment and analysis minimizes the steps for sample pretreatment, eliminating errors arising from sample transfer and solvent extraction in conventional methods. This has consequently improved the detection efficiency and accuracy. The spiked recoveries of the method were between 90.5% and 115.2%, with relative standard deviations ranging from 0.6% to 8.1%. Short-term monitoring of airport ambient air and aircraft cabin air revealed that benzene homologues concentrations significantly increased during airport peak flight hours and the initial stage of aircraft takeoff, and gradually decreased during the flight. Based on concentration ratios and correlation analyses, we inferred that airport ambient air homologues primarily originated from aviation fuel combustion and ground transportation exhaust, while cabin air homologues stemmed from interior material volatilization, outdoor air circulation/recirculation, and fuel vapor permeation. This study presents a novel technical approach for airport and cabin air quality monitoring, providing scientific evidence for relevant environmental management and health risk assessments.

Received 17th March 2025
Accepted 2nd July 2025

DOI: 10.1039/d5ra01898f

rsc.li/rsc-advances

1 Introduction

According to the latest report from the International Air Transport Association (IATA, 2024), the global number of commercial flights surged from 36.5 million in 2019 to 42.3 million in 2023, representing a compound annual growth rate of 3.7%. In particular, the Asia–Pacific region witnessed a significant increase, with the flight volume growing from 12.8 million to 15.6 million during the same period. This rapid growth in air transport has heightened concerns over air quality in airports and aircraft cabins. Benzene homologues (benzene, toluene, ethylbenzene, xylenes, *etc.*), classified as volatile organic compounds (VOCs), pose significant health risks due to their carcinogenicity, teratogenicity, and persistent toxicity, making them a global research priority in environmental and public health.[1,2] Airport environments are major emission sources of these pollutants, driven by aircraft/ground vehicle exhaust, fuel evaporation, cargo operations, and nearby industrial activities, with concentrations influenced by flight frequency and meteorological conditions.[3–7] Within aircraft cabins, emissions arise from interior materials, fuel vapor permeation, and recirculated air systems,[8–11] often exceeding WHO indoor air quality guidelines (2016). Chronic exposure to low-level benzene homologues is linked to respiratory and neurological damage in both crew members and

[a]*Civil Aviation Flight University of China, Research Center for Civil Aviation High Altitude Aviation Medicine, Guanghan 618307, Sichuan, China. E-mail: jiangjw1129@126.com*

[b]*Sichuan Center for Disease Control and Prevention, Chengdu 610041, Sichuan, China. E-mail: yuan2xx@126.com*

[c]*China Eastern Airlines Sichuan Branch, Chengdu 610225, Sichuan, China*

[d]*Civil Aviation Flight University of China, College of Airport, Guanghan 618307, Sichuan, China*

† Electronic supplementary information (ESI) available. See DOI: https://doi.org/10.1039/d5ra01898f

‡ These authors contributed equally to this work.

passengers,[12–14] prompting WHO to list them as priority pollutants (2021). Current research has focused mainly on field sampling and monitoring of benzene homologues in industrial zones and urban atmospheres. Systematic research on special environments such as airports and aircraft cabins remains relatively scarce,[14–16] which primarily concentrate on portable VOCs monitoring methodologies and modeling analysis.[15–18] Thus, advanced analytical methods are critical for aviation air quality assessment and health protection.

Two-stage thermal desorption (TTD) coupled with gas chromatography (GC)-flame ionization detector (FID)/gas chromatography-mass spectrometry (GC-MS), Especially TTD-GC-FID has emerged as a powerful tool for VOC analysis, offering high enrichment efficiency, solvent-free operation, and low sample consumption.[19–23] Compared to solvent-based methods, TTD enhances detection limits *via* primary desorption and cold trap focusing while eliminating solvent interference.[24–28] Successful applications include indoor/urban air,[29–34] industrial emissions/industrial ambient air,[35–40] vehicle environments/vehicle emissions,[41–44] healthcare settings,[45] and breath gas.[46,47] Therefore, the application of TTD-GC in the detection of benzene-series compounds within aircraft cabin environments demonstrates several unique advantages. First, the solvent-free pretreatment process eliminates secondary contamination risks associated with conventional solvent-based methods. Second, the technique exhibits exceptional resistance to analytical interference. By optimizing instrumental analytical parameters and thermal desorption conditions, effectively mitigating interference from water vapor, CO_2, and high-boiling compounds.

This study developed a standardized TTD-GC protocol for the simultaneous detection of eight benzene homologues in airport ambient and aircraft cabin air. Sampling procedures were optimized for aviation environments, and analytical parameters were rigorously validated. Comparative analysis of functional zones (runway zone, terminal building zone, apron zone, auxiliary zone) in general aviation and commercial transportation airports, as well as aircraft cabins, revealed distinct distribution patterns of benzene homologues. These findings elucidate the emission sources and influencing factors, providing a methodological foundation for targeted pollution control in aviation ecosystems.

2 Experimental and methodology

2.1 Experimental

2.1.1 Instruments and reagents. The following instruments were used: a 7890A gas chromatograph equipped with a hydrogen flame ionization detector (Agilent Technologies, USA); a hydrogen generator (Peak, UK); a Unity Series 2 two-stage desorber (Markes, UK); a LAB-T220 aging instrument (Guangzhou Appinno Instrument Co., Ltd, China); Tenax-TA adsorption tubes and 0.22 μm polytetrafluoroethylene membrane (Markes, UK); a DB-WAX capillary column (30 m × 0.25 mm × 0.25 μm); a gas preparation instrument for preparing standard series by liquid external standard method (equipped with a high-purity nitrogen flow regulator); an air sampling pump (flow range: 0.1–1.0 L min^{-1}, Wuhan Tianhong Instruments Co., Ltd, China); a multi-range electronic soap film flow meter (Beijing Municipal Institute of Labour Protection, China); pipettes with volume ranges between 0.5 and 1000 μL (Biohit, Finland); and 10.0 μL microinjectors (Shimadzu, Japan).

A certified mixed standard solution of eight benzene homologues in methanol (benzene, toluene, ethylbenzene, *p*-xylene, *m*-xylene, *o*-xylene, styrene and *p-tert*-butyltoluene, 1000 ng μL^{-1}) was purchased from Beijing Tanmo Quality Testing Technology Co., Ltd; methanol was purchased from Fisher Scientific (USA).

2.1.2 Sample collection. This study selected a commercial transportation airport and a general aviation airport as atmospheric sampling sites. Corresponding types of commercial transportation aircraft and flight training aircraft were chosen for cabin air sampling. To ensure spatial representativeness, airport sampling covered pollution source zones, diffusion zones, and background sites. Cabin sampling targeted high-density passenger areas and pollution-sensitive zones. For temporal representativity, airport sampling was conducted in three time windows: morning (6:00–9:00), noon (12:00–15:00), and evening (18:00–21:00). Cabin sampling covered different flight cycles, including weekdays and weekends. Based on airport functional layouts, four representative sampling points were established per airport. The runway area included three points at 50 m, 200 m, and 500 m from the runway center line. The terminal building area covered three points: departure entrance (De), security checkpoint (Sc), and waiting lounge (Wl). The apron area included four points, with two each in cargo aprons (Ca) and passenger aprons (Pa). The auxiliary area comprised two points: fuel storage zone (Fsz) and maintenance hangar (Mh). Additionally, three meteorological control points were set in upwind background areas per airport. Pre-conditioned Tenax-TA adsorption tubes were connected to air sampling pumps. Flow rates were calibrated using a soap film flowmeter. Air samples were collected at 200 mL min^{-1} for 30 minutes. Sampling height was fixed at 1.5 m, aligning with the human breathing zone. Temperature and atmospheric pressure were recorded for standardized volume conversion.

Three sampling points were set per cabin. The front cabin point was located in the first-class seat area, 2 m from the cabin door. The mid-cabin point was in the central economy section near the emergency exit. The rear cabin point covered the tail galley and lavatory area. Each transport aircraft had three fixed points, while smaller training aircraft used a single sampling point. Sampling covered 10 flights per category, using the same aircraft model with an age of ≤5 years (mainly based on two considerations: the higher volatility of interior materials and ensuring the controllability of the method variables). To mitigate cabin pressure effects, samples were collected at 200 mL min^{-1} for 30 minutes, covering takeoff, landing, and selected cruising periods. Sampling avoided strong airflow zones, such as air conditioning vents. Sampling heads were vertically fixed on tripods. For cabin sampling, samplers were mounted on seatback brackets, avoiding direct passenger exhalation. Sampling height was 1.2 m above the cabin floor,

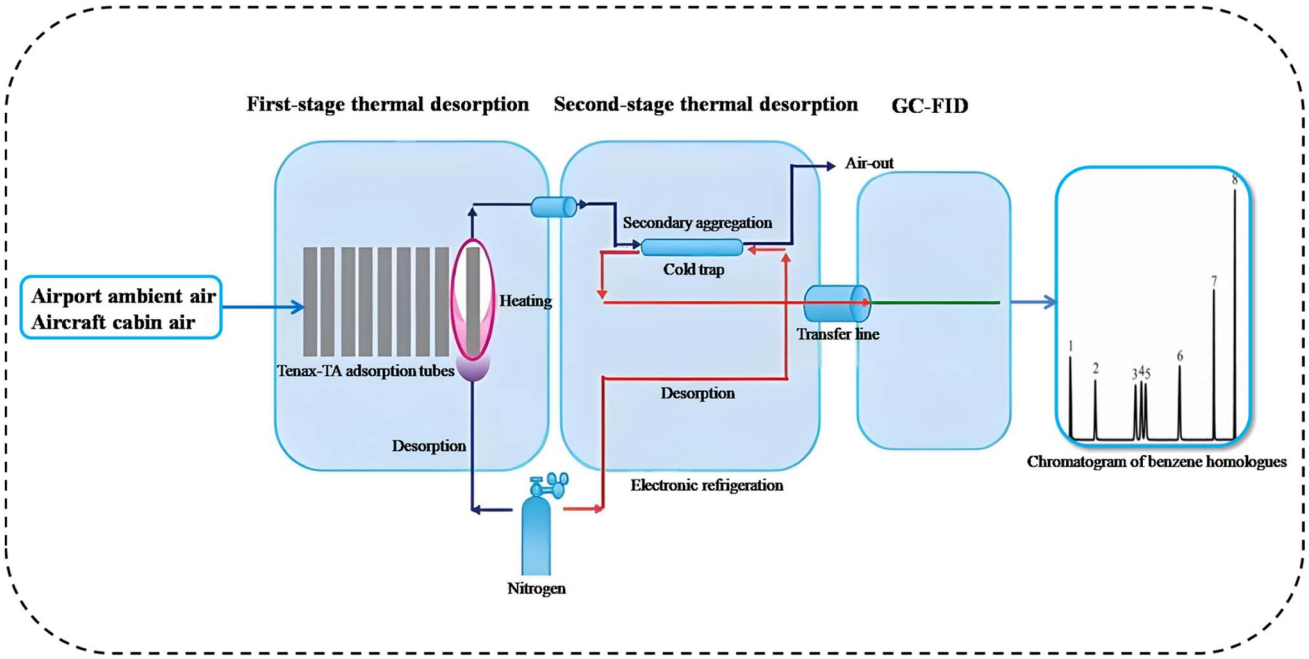

Fig. 1 Schematic diagram of TTD-GC-FID system.

matching the seated passenger breathing height. Domestic flights with a duration of ≥2 h were selected, maintaining a cabin pressure of 0.8 atm during cruise.

Post-sampling, tubes were sealed with two-piece threaded stainless steel caps, labeled with unique codes, and transported in containers maintained at ≤4 °C using dry ice to avoid vibration and high-temperature exposure. All samples were stored at −20 °C in the dark and underwent thermal desorption analysis within 7 days of arrival at the laboratory.

2.1.3 Two-stage thermal desorption and instrumental analysis conditions. As shown in Fig. 1, the sorbent tube was mounted on the desorber for first-stage thermal desorption under a non-split mode (all desorbed gas enter the cold trap for secondary aggregation) at a desorption nitrogen flow rate of 90 mL min^{-1}, with the temperature increased at a rate of 100 °C min^{-1} from room temperature to 320 °C and held at 320 °C for 10 minutes. Cold trapping was performed under a split mode with a split ratio of 20 : 1, with the cold trap temperature held at 0 °C for 0.8 minutes, then increased at a rate of 100 °C s^{-1} to 300 °C and held at 300 °C for 5 minutes during second-stage thermal desorption. The valve and transmission line maintained at 200 °C.

Benzene homologues compounds were separated on a DB-WAX capillary column (30 m × 0.25 mm × 0.25 μm). The column temperature was held at 60 °C for 7 minutes and then programmed at a rate of 30 °C min^{-1} to 150 °C, followed by post-run at 230 °C for 10 minutes. The carrier gas flow rate was 1.0 mL min^{-1}, the FID temperature was 300 °C, and the injection port temperature was 240 °C.

2.1.4 Quality control. Tenax-TA tubes were pre-conditioned before use. Used tubes underwent a 2-hour nitrogen purge at 320 °C, whereas new tubes underwent thermal activation for 3 hours at 320 °C. Activated tubes were capped with two-piece threaded stainless steel seals to prevent particle interference and stored in 4 °C desiccators. Field blanks, constituting 20% of total tubes, were analyzed. Target compounds in blanks were required to remain below the detection limits; otherwise, tubes were re-activated.

Sampling avoided strong airflow zones, such as air conditioning vents. Sampling heads were vertically fixed on tripods. For cabin sampling, samplers were mounted on seatback brackets, avoiding direct passenger exhalation. Sampling commenced 10 minutes before takeoff, with continuous flow rate monitoring. Galley sampling excluded meal service periods to avoid interference from VOC emission peaks. Each sampling batch included one field blank per point. Parallel samples accounted for at least 10% of each batch, which involved duplicate sampling per point. Before analysis, a mid-concentration calibration standard was analyzed per batch, requiring $a \leq 20\%$ relative error compared to the calibration curve.

2.2 Methodology

2.2.1 Selection of chromatographic conditions. Considering that the injection port temperature cannot be lower than the thermal desorption transfer line temperature, as desorbed analytes would otherwise condense before entering the column and compromise separation. Moreover, to ensure complete vaporization of the eight benzene homologues without thermal decomposition, which could reduce recovery. Therefore, the effects of different injection port temperatures (200, 220, 240, 260 and 280 °C) on the total peak area of the eight benzene homologues were investigated with all other conditions kept unchanged. The results showed that, when the injection port

temperature was 240 °C, benzene homologues were gasified to the maximum extent, and the largest total peak area was obtained. Since ethylbenzene, *p*-xylene, *m*-xylene and *o*-xylene cannot be easily separated, and the fact that constant temperature analysis can cause peak broadening of high boiling point compounds such as styrene and *p-tert*-butyltoluene. Therefore, this study chose to program the temperature of the chromatographic column. In addition, the column temperature and flow rate will both have an impact on the separation effects and analytical run time. To further shorten the run time while ensuring the eight benzene homologues can be well separated, a two-factor three-level orthogonal test was carried out to optimize the column temperature program and the flow rate. The results showed that, when the column flow was maintained at 1.0 mL min^{-1} and the column temperature was programmed at a ramp of 30 °C min^{-1} from an initial temperature of 60 °C (held for 7 minutes) to 150 °C, the eight benzene homologues could be well separated, and the obtained total peak area was the largest while the analytical run time was the shortest. These chromatographic conditions were therefore adopted.

2.2.2 Selection of two-stage thermal desorption conditions

2.2.2.1 First-stage thermal desorption temperature. Boiling points of the eight benzene homologues differ significantly. Ethylbenzene, xylene and, particularly, *p-tert*-butyltoluene (boiling point: 193 °C) require a high desorption temperature, while the filler of Tenax-TA adsorbent tubes requires the experimental temperature to be lower than 350 °C. Meanwhile, considering that the temperature is too high, the compound will undergo thermal decomposition. Therefore, the desorption effects of benzene homologues (based on the total peak area of the eight benzene homologues) at different desorption temperatures (240, 260, 280, 300, 320 and 340 °C) were investigated. Fig. S1 (ESI)†- depicts the relationship between desorption temperature and total peak area. The results showed that the total peak area increased with the desorption temperature when it was below 320 °C but leveled off at higher temperatures. Therefore, the first-stage desorption temperature was optimized at 320 °C.

2.2.2.2 Desorption time. Excessively short desorption time will compromise the desorption efficiency of benzene homologues. Furthermore, time is required for raising the desorption temperature to the target value. However, prolonged thermal desorption time may elevate background impurities. Therefore, the effects of different desorption times (4, 6, 8, 10, and 12 minutes) on the total peak area of the eight benzene homologues were investigated. The results showed that the total peak area increased with the desorption time when it was below 10 minutes but plateaued at longer durations. Therefore, a desorption time of 10 minutes was selected as the optimal.

2.2.2.3 Cold trapping temperature. The cold trapping temperature refers to the cryogenic focus temperature during two-stage thermal desorption, achieved *via* a Peltier-cooled trap. In two-stage thermal desorption analysis, cold trapping temperature is a critical parameter whose core function is to improve chromatographic separation efficiency and detection sensitivity of target analytes through low-temperature enrichment and focusing effects. Given that the capture and desorption efficiencies of the eight benzene homologues vary with temperature, a systematic investigation was conducted. A too-high cold trapping temperature may result in insufficient analyte focusing and reduced recovery, whereas an excessively low temperature risks ice blockage due to ambient humidity. Thus, the effects of different cold trapping temperatures (−30, −20, −10, 0, 10, and 20 °C) on desorption efficiency were evaluated. The total peak area reached a maximum at 0 °C, leading to the selection of 0 °C as the optimal cold trapping temperature.

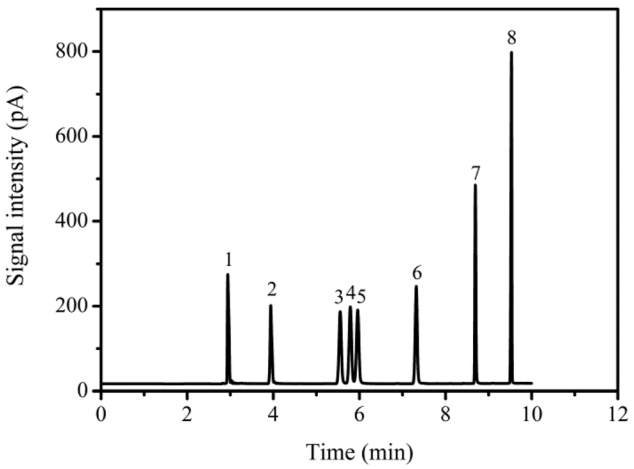

Fig. 2 Chromatogram of standard solution of eight benzene homologues ((1). benzene; (2). toluene; (3). ethylbenzene; (4). *p*-xylene; (5). *m*-xylene; (6). *o*-xylene; (7). styrene; (8). *p-tert*-butyltoluene).

2.2.2.4 Second-stage thermal desorption temperature. To ensure complete desorption of benzene homologues, prevent thermal decomposition of target compounds, and remove residual matrix from the quartz tube, the effects of different second-stage desorption temperatures (280, 300, 320 and 340 °C) on the desorption efficiency were investigated while maintaining the first-stage desorption temperature (320 °C), desorption time (8 minutes), and cold trapping temperature (0 °C) constant. The results showed that the total peak area reached a maximum at 300 °C and did not significantly change at higher temperatures. Thus, the second-stage desorption temperature was optimized at 300 °C.

3 Results and discussion

3.1 Linearity, limit of detection and limit of quantification of TTD-GC

Using a pipette, 10 μL, 50 μL, 100 μL, 250 μL, 500 μL and 1000 μL of mixed standard solution were transferred to sample vials and dilute with methanol to 1.0 mL to produce 10 ng μL^{-1}, 50 ng μL^{-1}, 100 ng μL^{-1}, 250 ng μL^{-1}, 500 ng μL^{-1} and 1000 ng μL^{-1} mixed standard working solutions. Standard curves were plotted by liquid external standard method. Under a 90 mL min^{-1} nitrogen flow, an aged sorbent tube was connected to a liquid standard based gas preparation instrument, and, using a micro-injector, 1.0 μL of each standard concentration point was injected into the gas preparation instrument and purged for

Table 1 Linear equations, linear correlation coefficients, detection limits and limits of quantification

Compound	Linear equations	Correlation coefficients	Detection limits (ng m^{-3})	Limits of quantification (ng m^{-3})
Benzene	$y = 0.47139x + 20.22435$	0.999	41	164
Toluene	$y = 1.16810x - 25.10382$	0.999	48	192
Ethylbenzene	$y = 1.26377x - 19.31280$	0.999	70	280
P-Xylene	$y = 1.20156x - 16.03786$	0.998	64	256
M-Xylene	$y = 1.20024x - 15.23678$	0.999	59	236
O-Xylene	$y = 1.27001x - 15.38976$	0.999	69	276
Styrene	$y = 1.25823x - 13.37982$	0.999	102	408
P-tert-Butyltoluene	$y = 1.20997x + 2.22546$	0.999	108	432

Table 2 Desorbed efficiency and stability of eight benzene homologues

			Measured value (ng)			
Compound	Desorbed efficiency (%)	RSD (%, $n = 7$)	5 d	10 d	15 d	20 d
Benzene	94.5	6.2	243	238	233	230
Toluene	98,7	7.9	245	239	237	230
Ethylbenzene	99,1	8.6	248	250	241	237
P-Xylene	99.7	6.1	250	248	244	246
M-Xylene	100.5	2.1	248	245	250	246
O-Xylene	102.1	1.2	252	250	249	237
Styrene	99.7	1.0	248	244	251	238
P-tert-Butyltoluene	105.9	8.3	250	249	240	242

5 minutes, followed by two-stage thermal desorption-gas chromatography analysis. Analytes were identified by retention time. Fig. 2 displays a chromatogram of the eight benzene homologues, demonstrating their excellent separation. Standard curves for the eight homologues were constructed with peak areas as the ordinate and concentrations as the abscissa. The calibration curve for benzene is shown in ESI Fig. S1.† The linear correlation coefficients of the eight benzenes were obtained. The limit of detection was defined as three times the signal-to-noise ratio, and the limit of quantification as 4 times the limit of detection, based on a sample volume of 6 L. The results are presented in Table 1. It can be known that good linearity was obtained over the range of 10–1000 ng for the eight benzene homologues. Limits of detection ranged between 41 ng m^{-3} and 108 ng m^{-3}, and the limits of quantification ranged between 164 ng m^{-3} and 432 ng m^{-3}.

3.2 Thermal desorption efficiency and stability test

Using a 10 μL micro-injector, 1.0 μL of 250 ng μL^{-1} standard solution was injected into the gas preparation instrument (ultrapure nitrogen flow rate: 90 mL min^{-1}), and the analytes were enriched in seven pre-aged Tenax-TA sorbent tubes. Desorption efficiency test results are presented in Table 2. The desorption efficiency of the eight benzene homologues ranged from 94.5% to 105.9%, with relative standard deviations (RSDs) ranging from 1.0% to 8.6%. These results indicate that, under appropriate experimental conditions, the eight benzene homologues adsorbed on Tenax-TA sorbent tubes can be completely desorbed. Twelve aged Tenax-TA sorbent tubes were

Table 3 Recoveries and relative standard deviations of eight benzene homologues

	Recoveries (%)			Relative standard deviations (%)		
Compound	10 (ng μL^{-1})	250 (ng μL^{-1})	1000 (ng μL^{-1})	50 (ng μL^{-1})	250 (ng μL^{-1})	1000 (ng μL^{-1})
Benzene	90.5	100.3	98.8	5.3	0.6	4.8
Toluene	99.3	99.6	103.1	8.1	5.3	4.7
Ethylbenzene	100.5	99.7	102.1	3.4	2.8	0.6
P-Xylene	110.2	109.1	99.9	8.0	7.4	5.6
M-Xylene	115.2	98.8	102.3	0.6	8.1	2.1
O-Xylene	99.8	107.7	102.1	0.7	2.3	5.2
Styrene	91.1	99.6	103.5	0.6	8.1	4.9
P-tert-Butyltoluene	99.8	107.6	103.4	7.6	6.9	0.9

Table 4 The average and total concentrations of eight benzene homologues in the commercial transportation airport ambient air in December 2024 (μg m^{-3})[a]

	Runway area									Terminal building area									Apron area						Auxiliary area					
	Morning			Noon			Evening			Morning			Noon			Evening			Morning		Noon		Evening		Morning		Noon		Evening	
Compound	50 m	200 m	500 m	50 m	200 m	500 m	50 m	200 m	500 m	De	Sc	Wl	De	Sc	Wl	De	Sc	Wl	Ca	Pa	Ca	Pa	Ca	Pa	Fsz	Mh	Fsz	Mh	Fsz	Mh
Benzene	29.6	13.6	9.8	15.3	8.3	5.4	36	20.2	12.9	6.0	1.2	4.3	3.5	1.0	2.4	7.3	1.6	4.6	2.7	2.5	2.1	0.9	3.3	2.7	9.3	9.9	9.2	9.5	9.7	9.9
Toluene	22.8	10.3	10.2	19.8	8.9	9.0	21.3	12.1	12.3	7.1	1.2	2.6	5.3	1.3	1.9	8.0	1.3	2.7	2.0	0.9	1.5	0.3	2.4	1.1	7.1	9.4	5.7	5.4	9.8	9.9
Ethylbenzene	19.9	8.1	8.0	15.7	7.7	6.6	20.6	9.2	8.5	4.7	1.0	1.6	4.1	0.9	1.1	5.5	1.0	1.5	3.1	1.7	2.7	1.6	3.4	1.7	3.6	8.9	3.2	5.8	3.9	9.7
p-Xylene	14.4	6.7	5.4	13.7	7.0	5.5	14.7	7.6	6.1	4.2	—	0.3	3.8	—	0.2	4.7	—	0.4	2.8	1.4	2.4	1.4	3.1	1.5	1.8	3.2	1.5	1.5	2.6	4.3
m-Xylene	13.8	3.9	0.07	12.6	3.5	—	13.9	4.7	0.1	3.9	0.2	—	3.5	0.1	—	4.4	0.3	—	2.9	0.9	2.6	0.7	3.2	1.0	1.0	2.5	0.7	1.0	1.6	3.2
o-Xylene	2.4	—	—	1.7	—	—	2.6	—	—	2.6	—	—	2.4	—	—	2.9	—	—	3.1	1.2	2.2	1.1	3.3	1.4	1.1	2.7	0.7	1.0	1.3	3.1
Styrene	12.2	6.5	4.2	9.3	4.1	2.8	14.2	8.2	5.2	2.5	0.7	1.0	2.0	0.6	0.5	3.3	0.8	1.0	3.7	1.9	3.1	1.4	3.9	2.2	0.7	0.9	0.2	0.3	0.9	1.3
p-tert-Butyltoluene	8.3	4.9	2.0	5.2	2.7	0.8	9.0	4.3	1.1	1.9	0.7	1.0	1.3	0.5	0.5	1.9	0.6	1.1	3.0	1.7	2.1	1.1	3.4	1.8	—	0.2	—	—	0.2	—
∑eightbenzene homologues	123	54	40	93	42	30	132	66	46	33	5	11	26	4	6.6	38	6	11	23	12	19	9	26	13	25	38	21	25	30	41

[a] — not detected.

Table 5 The average and total concentrations of eight benzene homologues in the general aviation airport ambient air in December 2024 (μg m^{-3})[a]

	Runway area									Terminal building area									Apron area						Auxiliary area					
	Morning			Noon			Evening			Morning			Noon			Evening			Morning		Noon		Evening		Morning		Noon		Evening	
Compound	50 m	200 m	500 m	50 m	200 m	500 m	50 m	200 m	500 m	De	Sc	Wl	De	Sc	Wl	De	Sc	Wl	Ca	Pa	Ca	Pa	Ca	Pa	Fsz	Mh	Fsz	Mh	Fsz	Mh
Benzene	5.7	2.7	1.5	2.4	1.1	0.5	6.4	3.2	1.7	1.3	0.2	0.5	0.8	0.2	0.5	1.5	0.3	0.6	1.5	1.2	1.1	0.8	1.7	1.4	2.0	1.6	1.8	1.1	2.4	1.9
Toluene	4.6	2.0	1.2	2.5	1.0	0.6	5.2	2.5	1.7	1.4	0.2	0.4	1.0	0.1	0.2	1.6	0.4	0.5	1.1	0.6	0.9	0.1	1.2	0.8	2.7	1.9	2.8	1.5	3.0	2.0
Ethyl benzene	3.7	1.7	0.8	1.6	0.6	0.3	4.0	2.1	1.2	0.9	0.2	0.3	0.7	0.1	0.2	1.1	0.3	0.4	1.6	1.3	1.4	0.9	1.8	1.4	0.4	1.9	0.2	1.8	0.6	2.5
P-Xylene	2.6	1.2	0.4	0.8	0.3	0.1	2.5	1.5	0.9	0.7	—	—	0.5	—	—	0.8	0.1	0.2	1.5	1.0	1.3	0.6	1.4	1.4	0.2	0.4	0.1	0.2	0.2	0.6
M-Xylene	2.5	0.7	—	0.9	0.3	—	3.6	0.8	0.2	0.6	0.1	—	0.5	—	—	0.8	0.2	0.1	1.5	0.8	1.3	0.4	1.5	1.1	0.1	0.2	—	0.3	0.3	0.4
O-Xylene	0.5	0.1	—	0.1	—	—	0.9	0.5	0.1	0.4	—	—	0.4	—	—	0.5	0.1	0.2	1.7	1.0	1.2	0.6	1.9	1.1	0.1	0.3	—	0.1	0.2	0.3
Styrene	2.2	1.1	0.6	0.5	—	—	3.0	1.8	1.1	0.4	—	0.2	0.3	—	—	0.6	0.2	0.3	1.9	1.4	1.6	0.8	2.0	1.6	—	0.2	—	—	0.2	0.3
P-tert-Buty ltoluene	1.3	0.5	0.3	0.2	—	—	2.1	0.8	0.7	0.4	0.2	0.2	0.2	0.1	0.2	0.4	0.3	0.3	1.6	1.3	1.2	0.7	1.5	1.5	2.0	0.2	1.8	—	2.5	0.2
∑eight benzene homo logues	23.1	10	4.8	9.0	3.3	1.5	27.4	13.2	7.6	6.1	0.9	1.6	4.4	0.5	1.1	7.3	1.9	2.6	12.4	8.6	10	4.9	13	10.3	7.5	6.7	6.7	5.0	9.4	8.2

[a] — not detected.

Table 6 The average and total concentrations of eight benzene homologues in the commercial and training aircraft cabin ambient air in June 2024 and December2024 (μg m^{-3})[a]

	Commercial aircraft cabin						Training aircraft cabin	
	December 2024			June 2024			December 2024	June 2024
Compound	Front cabin	Mid-cabin	Rear cabin	Front cabin	Mid-cabin	Rear cabin	Cabin	Cabin
Benzene	1.0	1.2	2.0	0.5	0.6	1.0	0.4	0.2
Toluene	0.7	0.6	1.4	0.3	0.4	0.8	0.3	0.2
Ethylbenzene	0.6	0.7	1.1	0.3	0.3	0.6	0.2	0.1
P-Xylene	0.3	0.4	0.8	0.1	0.2	0.4	0.1	—
M-Xylene	0.5	0.5	0.9	—	0.1	0.3	—	—
O-Xylene	0.4	0.6	1.0	—	0.2	0.4	0.2	0.1
Styrene	0.3	0.4	0.6	—	—	0.2	0.2	—
P-tert-Butyltoluene	—	0.2	0.4	—	—	—	0.2	—
∑eightbenzene homologues	3.8	4.6	8.2	1.2	1.8	3.7	1.6	0.6

[a] — not detected.

processed by the same method and stored at 4 °C refrigerator. On 5, 10, 15 and 20 days, three sorbent tubes were taken and analytes were determined by two-stage thermal desorption-gas chromatography. The results showed that the concentrations of the eight benzene homologues remained stable during the 20-day storage period of the Tenax-TA sorbent tubes in the refrigerator, with the loss rates within 10% at all time points. The results indicate that, with the Tenax-TA sorbent tubes stored under closed and low-temperature conditions, the eight benzene homologues are stable. Such factors as physical diffusion have no significant effect. Samples of the eight benzene homologues collected in Tenax-TA sorbent tubes can be stored for 20 days under the above conditions. The thermal desorption efficiency and stability are superior to the national standard method and other reported methods.

3.3 Penetration volume determination

Tenax-TA filler, a 2,6-diphenylfuran porous polymer resin, demonstrates excellent performance in adsorbing and thermally desorbing hydrocarbons. During sampling with Tenax-TA, breakthrough is identified when the analyte concentration in the outflow gas reaches 5% of the inflow concentration. In actual determination, two sorbent tubes may be connected in tandem to the sampling pump, and the sampling volume at which the content in the back tube accounts for 10% of the total is referred to as the penetration volume.[48] The sampling volume for all analytes should be controlled within the penetration volume. Using two sorbent tubes in tandem, 2 L, 4 L, 6 L and 7 L of air were collected. After sampling, the two tubes were connected to the gas outlet of the gas preparation instrument, and the contents of the eight benzene homologues in the front tube and the back tube were determined as described for the preparation of standard sample tubes. None of the eight benzene homologues was detected from the back tube when the sampled air volume was 2 L, 4 L or 6 L. Benzene, toluene and styrene were detected from the back tube when the sampled air volume was 7 L. Thus, the safe sampling volume was set at 6 L, which exceeds the reported 5 L.[48]

3.4 Method precision and accuracy

Before conducting the recovery experiments on previously sampled tubes, we performed blank analyses on identical sorbent tubes under the same experimental conditions. We also conducted precision evaluations on both blank tubes and samples with known concentrations. Furthermore, precision was evaluated by two operators on three different dates. The background concentrations were measured and subtracted from the sample concentrations to ensure accurate recovery calculations. Within the standard linear range, low-, medium- and high-concentration mixed standards were separately added seven pre-aged blank sorbent tubes and analyzed under experimental conditions described in Section 2.1.3, and relative standard deviations (RSDs) were calculated. Similarly, sampled sorbent tubes spiked with low-, medium- and high-concentration mixed standards and blank-spiked samples were analyzed under the same conditions, and spiked recoveries were calculated. The results are presented in Table 3. These results indicate that the spiked recoveries of this method ranged range from 90.5% to 115.2%, with RSDs ranging from 0.6% to 8.1%.

3.5 Sample analysis and pollution source analysis

Air samples from airport zones and aircraft cabins were collected in June 2024 and December 2024 using the methodology outlined in Section 2.1.2. The two-thermal desorption and instrument conditions for sample analysis were carried out using the method described in Section 2.1.3. Monthly average concentrations of eight benzene homologues and their total levels were analyzed in Tables 4–6, results from the commercial transportation airport and general aviation airport in June 2024

are shown in ESI Tables S1 and S2.† Winter (December) exhibited higher benzene homologue concentrations than summer (June) across all areas, attributed to the severe winter haze in the Sichuan Basin, which enhances organic pollutant adsorption onto fine particulate matter.[49,50] Additionally, the synergistic effects of limited meteorological diffusion, increased anthropogenic emissions, enclosed terrain, and weakened vegetation purification may also lead to significantly higher concentrations of benzene homologues in December compared to June.[50,51]

As shown in Tables 4 and 5, benzene homologues were detected in all airport zones due to aviation fuel combustion and ground vehicle emissions. At commercial airport runways, concentrations followed an exponential decay from the centerline, with benzene levels at 50 m being 2.9-fold higher than at 500 m. General aviation runways showed steeper gradients, reflecting inefficient fuel combustion in smaller aircraft. Peak benzene concentrations at commercial airports reached 36 μg m^{-3} (compared to the ambient air emission limit of 50 μg m^{-3}), while toluene accounted for over 19% of total homologues at general aviation sites, likely due to the decomposition of oxygenated fuel additives. Terminal areas exhibited 200% higher benzene homologues in the De (departure entrance) than in Wl (waiting lounge), linked to vehicle exhaust infiltration and baggage conveyor wear. Sc (security checkpoint) showed elevated benzene levels, likely from X-ray machine electronic component emissions. Ca (cargo aprons) had higher ethylbenzene than Pa (passenger aprons), presumably due to packaging solvent volatilization and refrigerants leakage. Fsz (fuel storage zone) showed continuous baseline pollution from tank venting, and Mh (maintenance hangar) contained complex homologue profiles due to the use of xylene-rich cleaning agents. Diurnal variations revealed that evening peaks at commercial airports were 11% higher than morning peaks, correlated with thermal accumulation and atmospheric inversion layers, while general aviation sites experienced midday concentration drops during flight training pauses.

As shown in Table 6, benzene homologues were detected in aircraft cabins, originating from secondary air pollution and material emissions (interior materials, seating fabrics, and luggage components). Rear cabins in commercial aircraft had twice the benzene concentration of front cabins, attributed to volatilization of restroom cleaning agents, galley heating emissions, and insufficient ventilation. Mid-economy sections showed elevated levels due to reduced air exchange rates from high passenger density. The result also revealed that cabin air in both commercial and training aircraft exhibited higher homologue concentrations during taxiing/takeoff than during cruising. This is because these phases involved frequent engine power shifts, incomplete fuel combustion, and fuel vapor permeation, compounded by reduced air circulation. Notably, *p-tert*-butyltoluene was detected for the first time in the aircraft cabin ambient air. This is likely due to the use of additives, adhesives, or polymers containing *p-tert*-butyltoluene in cabin interior materials, such as seat foam fillers, sound insulation materials, and decorative panels for seats. It is also possible that plastic components in the cabin, such as luggage racks, small table boards, vent decorations, *etc.*, were introduced with *p-tert*-butyltoluene during the synthesis.

4 Conclusion

This study establishes an analytical framework based on TTD-GC to resolve benzene homologues pollution patterns in airport-aircraft environments. Through coordinated optimization of thermal desorption parameters and chromatographic conditions, it overcomes the limitations of conventional environmental monitoring in analyzing complex matrices. Coordinated optimization of thermal desorption parameters and chromatographic conditions overcame limitations of conventional environmental monitoring in complex matrix analysis. The integrated pretreatment design achieved trace-level detection (LOD < 108 ng m^{-3}) with a streamlined workflow that reduced human error, demonstrating operational stability through RSDs of 0.6–8.1% in dynamic monitoring. Systematic investigation reveals the time-resolved evolution of benzene homologues evolution throughout aircraft operation cycles. Terminal areas exhibited pulsed concentration fluctuations strongly correlated with flight frequency and ground service activities, confirming synergistic contributions from incomplete aviation fuel combustion and ground mobile sources. Cabin monitoring identified threefold higher peak concentrations during takeoff than during cruising, elucidating the thermal emission kinetics of interior materials and pressure-induced permeation effects. Notably, based on preliminary data analysis, *p-tert*-butyltoluene showed distinct concentration patterns potentially associated with cabin material emissions, suggesting its candidacy as a marker for further investigation. The developed methodology establishes the technical foundations for formulating aviation environmental benchmarks and enables precise source tracking of volatile organic pollutants. These findings advance green airport initiatives and support evidence-based strategies for maintaining healthy cabin environments. Additionally, this approach extends to cross-sector pollutant monitoring solutions in confined spaces across rail transit and maritime systems. Future integration with portable TTD devices, high-resolution mass spectrometry, and AI algorithms could enable real-time VOCs monitoring and risk prediction in aviation environments.[52,53] These advancements facilitate coordinated environmental governance across transportation sectors under dual-carbon goals.

Data availability

The authors confirm that the data are present within the article.

Conflicts of interest

There are no conflicts of interest to declare.

Acknowledgements

This work was financially supported by Tibet Autonomous Region Science and Technology Support Program

(XZ202401ZY0016), the Fundamental Research Funds for the Central Universities (24CAFUC03086), Sichuan Province Science and Technology Support Program (2023YFQ0068, 2023ZYD0152), and Sichuan Center for Disease Control and Prevention Research Project (ZX202106).

References

1 Y. Deng, Y. Liu, Y. Deng, J. Cheng, Y. Zou and W. Luo, *In situ* sulfur-doped mesoporous tungsten oxides for gas sensingtoward benzene homologues, *Chin. Chem. Lett.*, 2024, **35**, 108898.

2 A. Nored, X. Fu, R. Qi, N. Batbaatar and C. Jia, Volatile organic compound (VOC) contamination in hotel rooms: apilot study to understand sources and health risks, *Int. J. Environ. Res. Public Health*, 2024, **21**, 1464.

3 M. Masiol and R. M. Roy, Harrison, Aircraft engine exhaust emissions and other airport-related contributions to ambient air pollution: A review, *Atmos. Environ.*, 2014, **95**, 409–455.

4 E. T. Turgut, M. Cavcar, O. Usanmaz, O. D. Yay, T. Dogeroglu and K. Armutlu, Investigating actual landing and takeoff operations for time-in-mode, fuel and emissions parameters on domestic routes in Turkey, *Transport. Res. Transport Environ.*, 2017, **53**, 249–262.

5 X. Bo, X. Xue, J. Xu, X. Du, B. Zhou and L. Tang, Aviation's emissions and contribution to the air quality in China, *Atmos. Environ.*, 2019, **201**, 121–131.

6 J. Christodoulakis, F. Karinou, M. Kelemen, G. Kouremadas, E. F. Fotaki and C. A. Varotsos, Assessment of air pollution from Athens international airport and suggestions for adaptation to new aviation emissions restrictions, *Atmos. Pollut. Res.*, 2022, **13**, 101441.

7 P.-G. Kamila and J. Remigiusz, Analysis of the Nicolaus Copernicus airport activity in terms of the flight operations impact on air pollution, *Energies*, 2021, **14**, 8236.

8 G. P. Brasseur, R. A. Cox, D. Hauglustaine, I. Isaksen, J. Lelieveld, D. H. Lister, R. Sausen, U. Schumann, A. Wahner and P. Wiesen, European scientific assessment of the atmospheric effects of aircraft emissions, *Atmos. Environ.*, 1998, **32**, 2329–2418.

9 R. Xu, J. Lang, S. Cheng, G. Wang and X. Yang, Exploration of the atmospheric pollutant emission inventory of mobile sources from Beijing capital international airport, *J. Saf. Environ.*, 2017, **17**, 1957–1962.

10 U. Kesgin, Aircraft emissions at Turkish airports, *Energy*, 2006, **31**, 372–384.

11 S. Fan, Control measures and efficiency of air pollutant from aircraft in USA, *Environ. Sci. Manage.*, 2011, **36**, 40–43.

12 V. Dedesh, A. Leutp and S. Boris, Aircraft emission research within ISTC project, *Air Space Eur.*, 2001, **3**, 244–246.

13 I. Ivo, F. Luca, A. Carla and F. Francesco, Airport related air pollution and health effects, *Epidemiol. Prev.*, 2014, **38**, 237–243.

14 S. L. Penn, T. Boone Scott, C. Harvey Brian, W. Heiger-Bernays, T. Yorghos, A. Sarav and J. Levy, Modeling variability in air pollution-related health damages from individual airport emissions, *Environ. Res.*, 2017, **156**, 791–800.

15 A. Gaeta, G. Cattani, A. D. M. di Bucchianico, A. De Santis, G. Cesaroni, C. Badaloni, C. Ancona, F. Forastiere, R. Sozzi, A. Bolignano and F. Sacco, Development of nitrogen dioxide and volatile organic compounds land use regression models to estimate air pollution exposure near an Italian airport, *Atmos. Environ.*, 2016, **131**, 254–262.

16 H. Anke, S. Adrian, E. Matthias and R. Martin, Aircraft noise, air pollution, and mortality from myocardial infarction, *Epidemiology*, 2010, **21**, 829–836.

17 W. Chen, Y. Liao, J. Zhou, F. Liu, M. Xu and Y. Wu, Study on calculation method of airport air pollution high temporal resolution emission inventory, *Environ. Monit. China*, 2022, **38**, 217–226.

18 Z. Zhou, C. Lu, Q. Tan, Y. Deng and Y. Bai, Emission Inventory and Spatial and Temporal Distribution Characteristics of Air Pollutant in Chengdu Shuangliu International Airport, *Environ. Monit. China*, 2018, **34**, 75–83.

19 C. Ou-Yang, Y. Huang, T. Huang, Y. Chen, C. Wang and J. Wang, Characterization of thermal desorption with the Deans-switch technique in gas chromatographic analysis of volatile organic compounds, *J. Chromatogr. A*, 2016, **1462**, 107–114.

20 H. Peng, S. Chen, W. Li, D. Wu and Y. Guan, A cryogen-free refrigerating preconcentration/thermal desorption instrument for on-line determination of volatile organic compounds in ambient air, *Chin. J. Anal. Chem.*, 2011, **39**, 1482–1486.

21 M. De Poli, T. Chenet, S. Felletti, D. Spadafora, A. Cavazzini and F. A. Franchina, Sorbent-based sampling with two-stage trapping/desorption coupled to comprehensive two-dimensional gas chromatography and mass spectrometry for terpenoids Profiling in cannabis, *Anal. Sci. Adv.*, 2025, **6**, e202400044.

22 M. S. Popov, N. V. Ul'yanovskii and D. S. Kosyakov, Direct quantification of 1,1-dimethylhydrazine transformation products in sandy soil by thermal desorption gas chromatography-Tandem mass spectrometry, *Microchem. J.*, 2024, **197**, 109833.

23 R. A. Wernis, N. M. Kreisberg, R. J. Weber, Y. Liang, J. Jayne, S. Hering and A. H. Goldstein, Development of an *in situ* dual-channel thermal desorption gas chromatography instrument for consistent quantification of volatile, intermediate-volatility and semivolatile organic compounds, *Atmos. Meas. Tech.*, 2021, **14**, 6533–6550.

24 K. J. Kiland, L. Martins, S. A. Borden, S. Lam and R. Myers, Stability of volatile organic compounds in thermal desorption tubes and in solution, *J. Breath Res.*, 2025, **19**, 026001.

25 N. Ramírez, A. Cuadras, E. Rovira, F. Borrull and R. M. Marcé, Comparative study of solvent extraction and thermal desorption methods for determining a wide range of volatile organic compounds in ambient air, *Talanta*, 2010, **82**, 719–727.

26 J. Lu, Y. Li, J. Li, S. Jing, T. An, H. Luo, C. Ma, H. Wang, Q. Fu and C. Huang, An online method for monitoring

atmospheric intermediate volatile organic compounds with a thermal desorption-gas chromatography/mass spectrometry, *J. Chromatogr. A*, 2022, **1677**, 463299.

27 Y. Chen, J. Qiu, K. Xu, H. Zhu, S. Zhang, X. Lu and X. Li, Development of a portable gas chromatograph-mass spectrometer embedded with a low-temperature adsorption thermal desorption module for enhanced detection of volatile organic compounds, *Analyst*, 2025, **3**, 470–480.

28 Y. Peng, X. Feng, Y. Feng, L. Li, Y. Chen and J. Yu, Optimization of two-stage thermal desorption combined with pentafluorophenyl hydrazine derivatization-gas chromatography/mass spectrometry analytical method of atmospheric carbonyl compounds, *Microchem. J.*, 2024, **197**, 109794.

29 F. Bachelier, M. Mascles, M. R. McGillen, J.-P. Amiet, B. Grosselin and V. Däele, Development, optimization and validation of automated volatile organic compound data analysis using an on-line thermal desorption gas chromatograph with dual detection and application to measurements in ambient air, *J. Chromatogr. A*, 2024, **1735**, 465327.

30 C. Veenaas, M. Ripszam and P. Haglund, Analysis of volatile organic compounds in indoor environments using thermal desorption with comprehensive two-dimensional gas chromatography and high-resolution time-of-flight mass spectrometry, *J. Sep. Sci.*, 2020, **43**, 1489–1498.

31 G. K. S. Wong, S. Jun Nga and R. D. Webster, Quantitative analysis of atmospheric volatile organic pollutants by thermal desorption gas chromatography mass spectrometry, *Anal. Methods*, 2013, **5**, 219–230.

32 S. Rovelli, A. Cattaneo, A. Fazio, A. Spinazzè, F. Borghi, D. Campagnolo, C. Dossi and D. M. Cavallo, VOCs measurements in residential buildings: quantification *via* thermal desorption and assessment of indoor concentrations in a case-study, *Atmosphere*, 2019, **10**, 57.

33 C. Raeppel, B. M. Appenzeller and M. Millet, Determination of seven pyrethroids biocides and their synergist in indoor air by thermal-desorption gas chromatography/mass spectrometry after sampling on Tenax TA passive tubes, *Talanta*, 2015, **131**, 309–314.

34 X. Lin, G. Sun, J. Zhao, L. Tang, S. Li and Y. Xie, UiO-66 selective enrichment integrated with thermal desorption GC-MS for detection of benzene homologues in ambient air, *J. Anal. Methods Chem.*, 2021, **2021**, 3138436.

35 N. Ramírez, R. M. Marcé and F. Borrull, Determination of volatile organic compounds in industrial wastewater plant air emissions by multi-sorbent adsorption and thermal desorption-gas chromatography-mass spectrometry, *Int. J. Environ. Anal. Chem.*, 2011, **91**, 911–928.

36 J. Sun, Q. Peng, Z. Peng, L. Qu, Z. Zhang, W. Liu and S. S. H. Ho, Ambient volatile organic compounds in a typical industrial city in southern China: impacts of aromatic hydrocarbons from new industry, *Sci. Total Environ.*, 2024, **954**, 176424.

37 M. Rosa Ras, R. M. Marcé and F. Borrull, Volatile organic compounds in air at urban and industrial areas in the Tarragona region by thermal desorption and gas chromatography–mass spectrometry, *Environ. Monit. Assess.*, 2009, **161**, 389–402.

38 C. Chang, T. Lin, Y. Lin, Y. Hua, W. Chu, T. Lin, Y. Lin and J. Wu, Comparison between thermal desorption tubes and stainless steel canisters used for measuring volatile organic compounds in petrochemical factories, *Ann. Occup. Hyg.*, 2016, **60**, 348–360.

39 C. Na, K. Vikrant, K. Kim and Y. Son, Continuous monitoring of adsorption onto activated carbon using sub-ppm level gaseous benzene as a model volatile organic compound based on an automated thermal desorption-gas chromatography/mass spectrometry approach, *Environ. Res.*, 2020, **182**, 109024.

40 M. R. R. Mallorquí, R. M. M. Recasens and F. B. Ballarín, Determination of volatile organic compounds in urban and industrial air from Tarragona by thermal desorption and gas chromatography-mass spectrometry, *Talanta*, 2007, **72**, 941–950.

41 N. Szymlet, L. Rymaniak and B. Kurc, Chromatographic analysis of the chemical composition of exhaust gas samples from urban two-wheeled vehicles, *Energies*, 2024, **17**, 709.

42 N. Turner, M. Jones, K. Grice, D. Dawson, M. Ioppolo-Armanios and S. J. Fisher, 13C of volatile organic compounds (VOCS) in airborne samples by thermal desorption-gas chromatography-isotope ratio-mass spectrometry (TD-GC-IR-MS), *Atmos. Environ.*, 2006, **40**, 3381–3388.

43 J. Wang, Y. Huang, Y. Bo, Y. Zhang and L. Zhang, Air pollution characteristics and human health risk assessment of underground parking garages in Xi'an, China, *Indoor Built Environ.*, 2022, **32**, 1–20.

44 C. Xie, Y. Li and M. Lan, Thermal desorption-gas chromatography/mass spectrometric analysis of volatile organic compounds emitted from automobile chair in thermal condition, *Chin. J. Anal. Chem.*, 2011, **39**, 265–268.

45 D. C. Vu, T. L. Ho, P. H. Vo, G. Carlo, J. A. McElroy, A. N. Davis, S. C. Nagelg and C.-Ho Lin, Determination of volatile organic compounds in child care centers by thermal desorption gas chromatography-mass spectrometry, *Anal. Methods*, 2018, **10**, 730–742.

46 K. Westphal, D. Dudzik, M. Waszczuk-Jankowska, B. Graff, K. Narkiewicz and M. Jan Markuszewski, Common strategies and factors affecting off-line breath sampling and volatile organic compounds analysis using thermal desorption-gas chromatography-mass spectrometry (TD-GC-MS), *Metabolites*, 2023, **13**, 8.

47 I. Belluomo, S. E. Whitlock, A. Myridakis, A. G. Parker, V. Converso, M. J. Perkins, V. S. Langford, P. Spanel and G. B. Hanna, Combining thermal desorption with selected ion flow tube mass spectrometry for analyses of breath volatile organic compounds, *Anal. Chem.*, 2024, **96**, 1397–1401.

48 D. Xu, C. Liu, A. Zhang, X. Dong, K. Han, G. Wang and Z. Tang, Tenax TA adsorption/thermal desorption/capillary

gas chromatography for monitoring BTX in the ambient air, *J. Hyg. Res.*, 2004, **33**, 425–427.

49 G. Lan and A. Lv, Analysis of characteristics and human exposure of BTX pollution in ambient air in winter, *Res. Environ. Sci.*, 2009, **22**, 40–46.

50 H. Zhao, Y. Ma, Y. Wang and Y. Zhu, Characteristics of particle mass concentrations and aerosol optical properties during a fog-haze event in Shenyang, *China Environ. Sci.*, 2015, **35**, 1288–1296.

51 K. Gu, S. Fan, H. Huang, H. Zhang, Y. Fan, F. Zu, B. Zhu and H. Li, Characteristics of polycyclic aromatic hydrocarbons (PAHs) in particles and the influence of foggy weather conditions during the winter in Nanjing, *China Environ. Sci.*, 2011, **31**, 1233–1240.

52 Y. Yin, J. He, L. Zhao, J. Pei, X. Yang, Y. Sun, X. Cui, C.-H. Lin, D. Wei and Q. Chen, Identification of key volatile organic compounds in aircraft cabins and associated inhalation health risks, *Environ. Int.*, 2022, **158**, 106999.

53 Q. Zhang, X. Zou, Q. Liang, Y. Zhang, M. I. Yi, H. Wang, C. Huang, C. Shen and Y. Chu, evelopment of dipolar proton transfer reaction mass spectrometer for real-time monitoring of volatile organic compounds in ambient air, *Chin. J. Anal. Chem.*, 2018, **46**, 471–478.